

Microwave power and chamber pressure studies for single-crystalline diamond film growth using microwave plasma CVD

Truong Thi Hien¹, Jaesung Park², Kwak Taeyeong³, Cuong Manh Nguyen⁴, Jeong Hyun Shim^{1,5,*}, Sangwon Oh^{4,†}

¹ Quantum Magnetic Sensing Group, Korea Research Institute of Standards and Science, Daejeon 34113, South Korea

² Tactile Standard Convergence Research Team, Korea Research Institute of Standards and Science, Daejeon 34113, South Korea

³ Tech University of Korea, Sangidaehak-ro, Siheung-si, Gyeonggi-do, 15073, Korea

⁴ Department of Physics, Ajou University, Gyeonggi-do, 16499, South Korea

⁵ Department of Applied Measurement Science, University of Science and Technology, Daejeon 34113, South Korea

Corresponding Author Email address: * jhshim@kriss.re.kr / † sangwonoh@ajou.ac.kr

Abstract

A smooth diamond film, characterized by exceptional thermal conductivity, chemical stability, and optical properties, is highly suitable for a wide range of advanced applications. However, achieving uniform film quality presents a significant challenge for the CVD method due to non-uniformities in microwave distribution, electric fields, and the densities of reactive radicals during deposition processes involving CH₄ and H₂ precursors. Here, we systematically investigate the effects of microwave power and chamber pressure on surface roughness, crystalline quality, and the uniformity of diamond films. These findings provide valuable insights into the production of atomically smooth, high-quality diamond films with enhanced uniformity. By optimizing deposition parameters, we achieved a root-mean-square (RMS) surface roughness of 2 nm, comparable to high-pressure, high-temperature (HPHT) diamond substrates. Moreover, these conditions facilitated the formation of a pure single-crystal diamond phase, confirmed by the absence of contamination peaks in the Raman spectra.

Keywords: microwave power, chamber pressure, surface roughness, uniformity film, high purity crystalline diamond, MP-CVD

1. Introduction

Diamond possesses remarkable properties, including large bandgap energy, high carrier mobility for both electrons and holes, high thermal conductivity, substantial infrared

transmittance, a low coefficient of friction, a robust structure, and chemical stability [1,2]. These attributes make it an outstanding material for a wide array of applications. Particularly, achieving a smooth and uniform surface in a diamond film is essential for optimizing its performance across various sectors, including optics, electronics, mechanics, chemistry, and biomedicine. Owing to the challenge of controlling impurities in natural and synthetic high-pressure, high-temperature (HPHT) diamonds, their practical applications have remained restricted [3]. In contrast, chemical vapor deposition (CVD) diamonds have emerged as promising alternatives within the realm of synthetic diamond production. These diamonds are synthesized through various methodologies such as HF-CVD, DC- and arc-plasma jets, DC-glow discharge, PCVD, and MP-CVD. Among these techniques, the MP-CVD method stands out for its recognized efficacy in yielding highly pure single-crystal diamonds (SCD) featuring atomically flat surfaces. However, a significant drawback of this approach lies in the inconsistency in diamond film quality observed between the center and the edge of the samples. This variation is attributed to factors such as non-uniform microwave distribution, ball-shaped plasma formation, and non-uniformity of the electric field and temperature across different regions of the substrate and within the chamber [4–8].

Various research strategies have been employed to address this issue, including the designs of chamber shapes and molybdenum substrate holders to enhance the uniformities of microwaves, electric fields, and temperature over the sample surface [9–12]. Additionally, studies on the effects of microwave power, chamber pressure, and gas composition ratio have significantly contributed to determining the optimal conditions to achieve a balance between the diamond deposition rate and the etching rate of non-diamond carbon products. These measures also ensure that diamond nucleations form primarily on the sample surface and that carbon atoms are consistently and continuously incorporated into the diamond lattice. Furthermore, these strategies minimize variations in the distribution of the CH_3^*/H radical ratio, electric field, and temperature across the sample surface from center to edge, thus improving the uniformity of the diamond film. In particular, the CH_3^* and H intermediate radicals produced from the decomposition of CH_4 and H_2 play a crucial role. The interaction of these radicals with the substrate initiates a series of reactions that facilitate the incorporation of carbon atoms into the diamond lattice, promoting the growth of the diamond film [13–21]. Tokuyuki et al. reported successful control of microwave power ranging from 3,800 to 4,200 W and variation of CH_4 concentrations from 0.4 to

32.0%, resulting in high-quality diamond films [22]. Vikharev et al. demonstrated that, under optimized microwave plasma CVD growth conditions, high-quality single-crystalline diamond films were obtained, devoid of non-epitaxial diamond crystallites, hillocks, or a polycrystalline diamond rim around the top surface [23]. The typical pressures for high-quality diamond film growth regimes in methane-hydrogen plasma are reported within 100–300 Torr [24–28]. Yang et al. have illustrated the non-uniform distribution of CH_3^*/H ratio, electric field, and temperature across the sample, resulting in disparate qualities of diamond film from the center to the periphery [29].

Furthermore, the variation in the CH_3^*/H ratio under different pressures, as noted by Michael et al., has been acknowledged to influence the deposition of diamonds [30]. Diamond films deposited using the MPCVD method typically exhibit uniform nucleation and growth mechanisms. High-quality films are achieved when carbon atoms are consistently and continuously integrated into the crystal lattice, resulting in a very smooth diamond film surface with minimal defects. Therefore, the quality of the diamond film is closely related to its surface roughness [7,31–33]. However, comprehensive research investigating the influences of both microwave power and chamber pressure on high-quality diamond film with atomic-level roughness, as well as the uniformity of diamond film surface at both the sample center and sample edge, has not been previously reported.

In this study, the MP-CVD deposition of diamond films was investigated using a CH_4 and H_2 mixture with a small addition of O_2 gas, under various conditions. Microwave power and chamber pressure were systematically varied to assess their impact on morphology uniformity, surface roughness, and crystalline quality at the center and edge of the samples. Observed trends in diamond film quality and uniformity are thoroughly analyzed and explained, offering a clearer understanding of the diamond growth process via the MP-CVD method.

2. Experiment

The diamond films were grown on (100)-oriented HPHT diamond substrates (from Elements Six Ltd.), $3 \times 3 \times 0.25 \text{ mm}^3$, using an MP-CVD system (SDS6350, Seki Diamond Ltd.). The HPHT diamond substrates were acid-cleaned, $\text{HNO}_3:\text{H}_2\text{SO}_4:\text{HClO}_4 = 1:1:1$ at $250 \text{ }^\circ\text{C}$ for 1 hour, before and after the growth, and the root mean square roughness (RMS) before the growth was approximately 1.96 nm over a $10 \times 10 \text{ }\mu\text{m}^2$ area. An outer diameter

of 50 mm and thickness of 3 mm Mo holder was used to hold the substrates. The holder had a $3.1 \times 3.1 \times 0.1 \text{ mm}^3$ recess, which held the substrate during the cooling down of the deposition process. H_2 , O_2 , and CH_4 gases with purities higher than 99.999%, were flown into the chamber, where their flow rates were controlled to be 490, 1, and 10 sccm, respectively. The existence of O_2 is known to improve diamond film quality [34]. The temperature at the surface of the substrates was monitored using a pyrometer (PRO2A, Williamson Corp.) through a quartz window at the top of the chamber. The Plasma-assisted CVD diamond growth process using CH_4 and H_2 as input gases is shown in Fig. 1. The morphology of the diamond films was examined using optical microscopy (OM, DM4M, Leica microsystems), field emission scanning electron microscopy (FE-SEM, FEI-Sirion 400 NC, Philips), and atomic force microscopy (AFM, XE7, Park system). Additionally, the films were characterized using Raman spectroscopy (WITec alpha300, Oxford instruments) and secondary ion mass spectrometry (SIMS, IMS 7f, CAMECA). The SIMS was used to confirm the deposition rate and concentration of impurities such as N and C.

3. Results and discussion

3.1. Effect of Microwave power

To understand the role of microwave power on the grown diamond film, we varied the microwave power from 2,700 W to 4,300 W and analyzed the surface using OM, SEM, AFM, and Raman spectroscopy. The OM images at different microwave power and the average temperature during the deposition are shown in Fig. 2a. The average temperature on the sample surface increases with the increase of microwave power. Noticeable differences in brightness were observed with lower microwave powers, ranging from 2,700W to 3,300W. These variations could be due to the surface imperfections and the increased grain boundaries, which affect brightness distribution within the images. Increasing the microwave power to 3,900W, resulted in the most uniform distribution brightness distribution. However, with microwave powers exceeding 3,900W, the sample's edge region gradually becomes darker. This inhomogeneity in the sample could be explained by the non-uniform distribution of radical density, electric field, and surface temperature between the sample's center and edge, as demonstrated in relevant studies [13,29,35,36].

To get a better understanding of the inhomogeneous brightness distribution, the morphological analysis of both the central and peripheral regions of the grown films was performed as depicted in Fig. 3. In the center of the films, the pit density decreases as the microwave power increases. These observations could be explained by the findings of James et al.; the growth of diamond films is influenced by the carbon incorporation into the lattice at activated sites, and the density of the activated sites increases with temperature [31]. Hence, the lower microwave power could lead to lower temperatures on the substrate surface, as shown in Fig. 2 (a), resulting in denser pits on the surface. However, the surface morphologies at the edges of the films show a different trend. Larger crystalline structures are dominant defects at the edges of the films. This could be explained by the radially increasing CH_3^*/H ratio due to the thin Mo holder as Yang et al. used. They calculated CH_3 and H density assuming a 3 mm-thick Mo holder and found the ratio of CH_3^*/H increases radially outward [29]. The increased CH_3^*/H ratio in the edges of the substrate increased the deposition rate over the etching by H, resulting in the lower pit density under the low microwave powers and larger crystalline structure under the high microwave powers in the edge of the films [25,34–38]. In our experiments, we found that the microwave power of 3,900W was an optimal power that balanced the density of activated sites and radially uneven CH_3^*/H ratio across the HPHT substrates.

The roughness of the diamond films at each microwave power was measured using AFM. The AFM images of a scan area of $10 \times 10 \mu\text{m}^2$ were taken at the center and edge of the films and shown in Fig. 4 (center) and Fig. 5 (edge). The RMS values of the surface roughness at the center and edge of the film decrease as the microwave power increases up to 3,900W and the roughness at the sample center remains unchanged with further increases in the power up to 4,300W. The smallest RMS at the center and edge of films was 2.0 nm when the microwave power was 3,900W. The smallest RMS values are comparable to the RMS of the bare HPHT substrate.

The Raman spectra at the center and edge of the grown diamond films from various microwave powers are shown in Fig. 6. We can find three different peaks in the spectra: the diamond phase (sp^3) peak at around $1,332.2 \text{ cm}^{-1}$, C-H bending at $1,416 \text{ cm}^{-1}$, and C-H stretching at $3,119 \text{ cm}^{-1}$ [39–45]. The Raman spectra of the microwave power of 3900W show a strong peak at $1,332.2 \text{ cm}^{-1}$ and are almost free of the other peaks, indicating that the grown diamond could be comparable to the HPHT substrate. This is a clear sign of a

high-quality single-crystal diamond (SCD) [15,46–48]. However, Raman spectra in the other conditions have C-H bending and stretching-related peaks. This could be explained by the higher etching rate at lower microwave power due to the decrease of the activated centers and enhanced CH_3^*/H ratio at higher microwave power [29,35,49,50].

The diamond peaks at the center and edge of samples grown in different microwave powers are expanded for clear comparison in Fig. 7. The Raman spectra of samples were in the 1331,8 to 1332,6 cm^{-1} range, with an insignificant shift within 1 cm^{-1} . The full width at half maximum (FWHM) of the peaks from the microwave powers are compared in Fig. 7 c. The FWHM decreases as the microwave power increases up to 3,900W and marginally decreases at the higher microwave powers. The growth rate of diamond films was found from SIMS measurements, which were performed only at the center of the films. The growth rate is approximately 1.2 $\mu\text{m}/\text{h}$, regardless of the microwave power.

3.2. Effect of chamber pressure

We also investigated the effect of chamber pressure in diamond film, such as morphology and composition. We fixed the microwave power at 3,900W and varied the pressure from 100 to 140 torr by utilizing pressure sensors and feedback systems while keeping the gas flow rates the same: 490 H_2 /10 O_2 /10 CH_4 . The temperature at the substrates stayed around 880 °C, as shown in Fig. 8a. The inhomogeneous brightness distribution occurred when the pressure was higher than 130 Torr, Fig. 8b-f.

To understand the uneven brightness distribution, we observed the grown diamond films using SEM, and the results are shown in Fig. 9. The density of the pits in the center and edge of the films increases as the pressure becomes higher than 130 Torr, and this observation agrees with Michael et al., which could be explained by the reduced CH_3^*/H ratio at higher pressure from 100 to 140 Torr [30]. The higher pit density in the center of the sample could be explained by the increased CH_3^*/H ratio at the edge of the film, as Yang et al. suggested [29].

The RMS roughness of the diamond films at each pressure was measured using AFM. The AFM images with a scan area of 10×10 μm^2 were taken at the center and edge of the films as the microwave cases and shown in Fig. 10 (center) and Fig. 11 (edge). The RMS values of the surface roughness suddenly deteriorate as the pressure becomes higher than 120 Torr, where the minimum RMS value of 2.0 nm was obtained at 120 Torr. This could be

explained by the reduced CH_3^*/H ratio at the higher pressure as Michael et al. suggested [30].

The Raman spectra at the center and edge of the grown diamond films from various pressure conditions are depicted in Fig. 12. The singular peak at $1,332.2\text{ cm}^{-1}$ in the case of 120 Torr confirms its high quality as the HPHT substrate [15,46]. However, Raman spectra from the other films revealed a C-H stretching defect peak at $3,119\text{ cm}^{-1}$ on both the central and edge areas [51]. Jiang et al. reported that defects formed at large crystals at low pressure enhanced C-H defect intensity [52]. Additionally, the higher pressure than the optimal pressure of 120 Torr would enhance the H/CH_3^* ratio, leading to increased surface termination by hydrogen atoms and intensifying the persistent vibration [53]

Fig. 13a and 13b illustrate the FWHM of Raman spectra at the central and edge surfaces of the samples, respectively. The Raman spectra of samples deposited in different chamber pressures were in the $1331,7$ to $1332,6\text{ cm}^{-1}$ range, appearing the negligible shift within 1 cm^{-1} . The FWHM of 7.86 cm^{-1} at the lower pressure is comparable to that of the HPHT substrate, whereas the FWHM at the higher pressure than 120 Torr becomes broad due to the defects in the diamond film, as seen in SEM and AFM measurements. The growth rate of diamond films was found from SIMS measurements, which were performed only at the center of the films. The growth rate is approximately $1.2\text{ }\mu\text{m/h}$, regardless of the pressure.

4. Summary

We have studied the influence of microwave power and chamber pressure in growing diamond films using OM, SEM, AFM, and Raman spectroscopy. The pit density, surface roughness, and crystalline quality of the diamond films were evaluated. The radially decreasing pit density from the morphology measurements was found, where the pit density could be explained by the radially increasing CH_3^*/H ratio due to the geometry of the Mo holder. By optimizing the microwave power and the pressure, we achieved the RMS roughness of 2 nm, which was comparable to that of the HPHT substrate. Additionally, we found the optimal microwave power and pressure conditions where the single diamond phase (sp^3) peak at $1,332.2\text{ cm}^{-1}$ existed without the other C-H peaks at $1,416$ and $3,119\text{ cm}^{-1}$ in the Raman spectra.

Declaration of competing interest

The authors declare that they possess no discernible competing financial interests or personal affiliations that might have conceivably influenced the research findings presented in this paper.

Acknowledgments

This research was supported by a grant (GP2024-0013) from Korea Research Institute of Standards and Science, the Institute of Information & communications Technology Planning & Evaluation (IITP) grant funded by the Korea government (MSIT)(2022-0-01026, RS-2023-00230717, No. 2021-0-00076), and a grant funded by the Ministry of Education (No. RS-2023-00285390).

References

- [1] J.W. Liu, M.Y. Liao, M. Imura, T. Matsumoto, N. Shibata, Y. Ikuhara, Y. Koide, Control of normally on/off characteristics in hydrogenated diamond metal-insulator-semiconductor field-effect transistors, *J Appl Phys* 118 (2015). <https://doi.org/10.1063/1.4930294>.
- [2] S. Koizumi, K. Watanabe, M. Hasegawa, H. Kanda, Ultraviolet emission from a diamond pn junction, *Science* (1979) 292 (2001) 1899–1901. <https://doi.org/10.1126/science.1060258>.
- [3] C.-S. Yan, Y.K. Vohra, H.-K. Mao, R.J. Hemley, Very high growth rate chemical vapor deposition of single-crystal diamond, 2002. www.pnas.org/cgi/doi/10.1073/pnas.152464799.
- [4] J. Liu, L.F. Hei, J.H. Song, C.M. Li, W.Z. Tang, G.C. Chen, F.X. Lu, High-rate homoepitaxial growth of CVD single crystal diamond by dc arc plasma jet at blow-down (open cycle) mode, *Diam Relat Mater* 46 (2014) 42–51. <https://doi.org/10.1016/j.diamond.2014.04.008>.
- [5] T.A. Railkar, W.P. Kang, H. Windischmann, A.P. Malshe, H.A. Naseem, J.L. Davidson, W.D. Brown, Critical review of chemical vapor-deposited (CVD) diamond for electronic applications, *Critical Reviews in Solid State and Materials Sciences* 25 (2000) 163–277. <https://doi.org/10.1080/10408430008951119>.
- [6] L.F. Hei, J. Liu, C.M. Li, J.H. Song, W.Z. Tang, F.X. Lu, Fabrication and characterizations of large homoepitaxial single crystal diamond grown by DC arc plasma jet CVD, *Diam Relat Mater* 30 (2012) 77–84. <https://doi.org/10.1016/j.diamond.2012.10.002>.
- [7] S. V Baryshev, M. Muehle, Scalable Production and Supply Chain of Diamond using Microwave Plasma: a Mini-review, n.d.
- [8] J. Zhang, J. Wang, G. Zhang, Z. Huo, Z. Huang, L. Wu, A review of diamond synthesis, modification technology, and cutting tool application in ultra-precision machining, *Mater Des* 237 (2024). <https://doi.org/10.1016/j.matdes.2023.112577>.

- [9] W. Cao, Z. Ma, H. Zhao, D. Gao, Q. Fu, The lateral outward growth of single-crystal diamonds by two different structures of microwave plasma reactor, *CrystEngComm* 24 (2022) 1010–1016. <https://doi.org/10.1039/d1ce01373d>.
- [10] F. Silva, K. Hassouni, X. Bonnin, A. Gicquel, Microwave engineering of plasma-assisted CVD reactors for diamond deposition, *Journal of Physics Condensed Matter* 21 (2009). <https://doi.org/10.1088/0953-8984/21/36/364202>.
- [11] J.J. Su, Y.F. Li, X.L. Li, P.L. Yao, Y.Q. Liu, M.H. Ding, W.Z. Tang, A novel microwave plasma reactor with a unique structure for chemical vapor deposition of diamond films, *Diam Relat Mater* 42 (2014) 28–32. <https://doi.org/10.1016/j.diamond.2013.12.001>.
- [12] A.K. Mallik, R. Rouzbahani, F. Lloret, R. Mary Joy, K. Haenen, Effect of substrate roughness on the nucleation and growth behaviour of microwave plasma enhanced CVD diamond films – a case study, *Functional Diamond* 3 (2023). <https://doi.org/10.1080/26941112.2023.2295346>.
- [13] V. Sedov, A. Martyanov, A. Altakhov, A. Popovich, M. Shevchenko, S. Savin, E. Zavedeev, M. Zaneskin, A. Sinogeykin, V. Ralchenko, V. Konov, Effect of substrate holder design on stress and uniformity of large-area polycrystalline diamond films grown by microwave plasma-assisted cvd, *Coatings* 10 (2020) 1–10. <https://doi.org/10.3390/coatings10100939>.
- [14] J. Achard, F. Silva, A. Tallaire, X. Bonnin, G. Lombardi, K. Hassouni, A. Gicquel, High quality MPACVD diamond single crystal growth: High microwave power density regime, *J Phys D Appl Phys* 40 (2007) 6175–6188. <https://doi.org/10.1088/0022-3727/40/20/S04>.
- [15] J. Sierra Gómez, J. Vieira, M.A. Fraga, E.J. Corat, V.J. Trava-Airoldi, Surface Morphology and Spectroscopic Features of Homoepitaxial Diamond Films Prepared by MWPACVD at High CH₄ Concentrations, *Materials* 15 (2022). <https://doi.org/10.3390/ma15217416>.
- [16] J. Weng, F. Liu, L.W. Xiong, J.H. Wang, Q. Sun, Deposition of large area uniform diamond films by microwave plasma CVD, *Vacuum* 147 (2018) 134–142. <https://doi.org/10.1016/j.vacuum.2017.10.026>.
- [17] A.P. Bolshakov, V.G. Ralchenko, G. Shu, B. Dai, V.Y. Yurov, E. V. Bushuev, A.A. Khomich, A.S. Altakhov, E.E. Ashkinazi, I.A. Antonova, A. V. Vlasov, V. V. Voronov, Y.Y. Sizov, S.K. Vartapetov, V.I. Konov, J. Zhu, Single crystal diamond growth by MPCVD at subatmospheric pressures, *Mater Today Commun* 25 (2020). <https://doi.org/10.1016/j.mtcomm.2020.101635>.
- [18] A.K. Mallik, S. Bysakh, R. Bhar, S.Z. Rotter, J.C. Mendes, Effect of Seed Size, Suspension Recycling and Substrate Pre-Treatment on the CVD Growth of Diamond Coatings, *Open Journal of Applied Sciences* 05 (2015) 747–763. <https://doi.org/10.4236/ojapps.2015.512071>.

- [19] B. Wang, J. Weng, Z.T. Wang, J.H. Wang, F. Liu, L.W. Xiong, Investigation on the influence of the gas flow mode around substrate on the deposition of diamond films in an overmoded MPCVD reactor chamber, *Vacuum* 182 (2020). <https://doi.org/10.1016/j.vacuum.2020.109659>.
- [20] S. V Baryshev, M. Muehle, Scalable Production and Supply Chain of Diamond using Microwave Plasma: a Mini-review, n.d.
- [21] Thin film diamond growth mechanisms, *Philosophical Transactions of the Royal Society of London. Series A: Physical and Engineering Sciences* 342 (1993) 209–224. <https://doi.org/10.1098/rsta.1993.0015>.
- [22] T. Teraji, M. Hamada, H. Wada, M. Yamamoto, T. Ito, High-quality homoepitaxial diamond (100) films grown under high-rate growth condition, in: *Diam Relat Mater*, 2005: pp. 1747–1752. <https://doi.org/10.1016/j.diamond.2005.06.021>.
- [23] A.L. Vikharev, M.A. Lobaev, A.M. Gorbachev, D.B. Radishev, V.A. Isaev, S.A. Bogdanov, Investigation of homoepitaxial growth by microwave plasma CVD providing high growth rate and high quality of diamond simultaneously, *Mater Today Commun* 22 (2020). <https://doi.org/10.1016/j.mtcomm.2019.100816>.
- [24] C.J. Widmann, W. Müller-Sebert, N. Lang, C.E. Nebel, Homoepitaxial growth of single crystalline CVD-diamond, *Diam Relat Mater* 64 (2016) 1–7. <https://doi.org/10.1016/j.diamond.2015.12.016>.
- [25] F. Silva, J. Achard, O. Brinza, X. Bonnin, K. Hassouni, A. Anthonis, K. De Corte, J. Barjon, High quality, large surface area, homoepitaxial MPACVD diamond growth, *Diam Relat Mater* 18 (2009) 683–697. <https://doi.org/10.1016/j.diamond.2009.01.038>.
- [26] Y. Mokuno, A. Chayahara, Y. Soda, H. Yamada, Y. Horino, N. Fujimori, High rate homoepitaxial growth of diamond by microwave plasma CVD with nitrogen addition, *Diam Relat Mater* 15 (2006) 455–459. <https://doi.org/10.1016/j.diamond.2005.11.046>.
- [27] Q. Liang, C. shiue Yan, Y. Meng, J. Lai, S. Krasnicki, H. kwang Mao, R.J. Hemley, Recent advances in high-growth rate single-crystal CVD diamond, *Diam Relat Mater* 18 (2009) 698–703. <https://doi.org/10.1016/j.diamond.2008.12.002>.
- [28] A.P. Bolshakov, V.G. Ralchenko, V.Y. Yurov, A.F. Popovich, I.A. Antonova, A.A. Khomich, E.E. Ashkinazi, S.G. Ryzhkov, A. V. Vlasov, A. V. Khomich, High-rate growth of single crystal diamond in microwave plasma in CH₄/H₂ and CH₄/H₂/Ar gas mixtures in presence of intensive soot formation, *Diam Relat Mater* 62 (2016) 49–57. <https://doi.org/10.1016/j.diamond.2015.12.001>.

- [29] B. Yang, Q. Shen, Z. Gan, S. Liu, Analysis of improving the edge quality and growth rate of single-crystal diamond growth using a substrate holder, *CrystEngComm* 21 (2019) 6574–6584. <https://doi.org/10.1039/c9ce01402k>.
- [30] M.N.R. Ashfold, Y.A. Mankelevich, Two-dimensional modeling of diamond growth by microwave plasma activated chemical vapor deposition: Effects of pressure, absorbed power and the beneficial role of nitrogen on diamond growth, *Diam Relat Mater* 137 (2023). <https://doi.org/10.1016/j.diamond.2023.110097>.
- [31] Thin film diamond growth mechanisms, *Philosophical Transactions of the Royal Society of London. Series A: Physical and Engineering Sciences* 342 (1993) 209–224. <https://doi.org/10.1098/rsta.1993.0015>.
- [32] S.J. Harris, Mechanism for diamond growth from methyl radicals, *Appl Phys Lett* 56 (1990) 2298–2300. <https://doi.org/10.1063/1.102946>.
- [33] M. Frenklach, S. Skokov, *Surface Migration in Diamond Growth*, 1996. <https://pubs.acs.org/sharingguidelines>.
- [34] T. Shimaoka, H. Yamada, Y. Mokuno, A. Chayahara, Oxygen Concentration Dependence in Microwave Plasma-Enhanced Chemical Vapor Deposition Diamond Growth in the (H, C, O, N) System, *Physica Status Solidi (A) Applications and Materials Science* 219 (2022). <https://doi.org/10.1002/pssa.202100887>.
- [35] S.A. Bogdanov, A.M. Gorbachev, A.L. Vikharev, D.B. Radishev, M.A. Lobaev, Study of microwave discharge at high power density conditions in diamond chemical vapor deposition reactor by optical emission spectroscopy, *Diam Relat Mater* 97 (2019). <https://doi.org/10.1016/j.diamond.2019.04.030>.
- [36] W.G.S. Leigh, J.A. Cuenca, E.L.H. Thomas, S. Mandal, O.A. Williams, Mapping the effect of substrate temperature inhomogeneity during microwave plasma-enhanced chemical vapour deposition nanocrystalline diamond growth, *Carbon N Y* 201 (2023) 328–337. <https://doi.org/10.1016/j.carbon.2022.09.036>.
- [37] S. Nad, Y. Gu, J. Asmussen, Growth strategies for large and high quality single crystal diamond substrates, *Diam Relat Mater* 60 (2015) 26–34. <https://doi.org/10.1016/j.diamond.2015.09.018>.
- [38] H. Yamada, A. Chayahara, S. Ohmagari, Y. Mokuno, Factors to control uniformity of single crystal diamond growth by using microwave plasma CVD, *Diam Relat Mater* 63 (2016) 17–20. <https://doi.org/10.1016/j.diamond.2015.09.016>.
- [39] T. Aizawa, T. Ando, K. Yamamoto, M. Kamo, Y. Sato, Surface vibrational studies of CVD diamond, n.d.

- [40] A.F.Azevedo, J.T. Matsushima, F.C. Vicentin, M.R. Baldan, N.G. Ferreira, Surface characterization of NCD films as a function of sp²/sp³ carbon and oxygen content, *Appl Surf Sci* 255 (2009) 6565–6570. <https://doi.org/10.1016/j.apsusc.2009.02.041>.
- [41] O. Kudryavtsev, R. Bagramov, A. Satanin, O. Lebedev, D. Pasternak, V. Filonenko, I. Vlasov, Raman fingerprints of ultrasmall nanodiamonds produced from adamantane, n.d.
- [42] C.L. Cheng, C.F. Chen, W.C. Shaio, D.S. Tsai, K.H. Chen, The CH stretching features on diamonds of different origins, *Diam Relat Mater* 14 (2005) 1455–1462. <https://doi.org/10.1016/j.diamond.2005.03.003>.
- [43] C.-L. Cheng, H.-C. Chang, J.-C. Lin, K.-J. Song, J.-K. Wang, *Direct Observation of Hydrogen Etching Anisotropy on Diamond Single Crystal Surfaces*, 1997.
- [44] S.P. Mehandru, A.B. Anderson, J.C. Angus, *Hydrogen binding and diffusion in diamond*, 1992. <http://journals.cambridge.org>.
- [45] R. Kakkar, *Vibrational Spectroscopy of Polyatomic Molecules*, in: *Atomic and Molecular Spectroscopy*, Cambridge University Press, 2015: pp. 231–262. <https://doi.org/10.1017/cbo9781107479999.007>.
- [46] P. Zhang, W. Chen, L. Zhang, S. He, H. Wang, S. Yan, W. Ma, C. Guo, Y. Wang, A. Surmenev, Evolution of High-Quality Homoepitaxial CVD Diamond Films Induced by Methane Concentration, (2021). <https://doi.org/10.3390/coatings>.
- [47] V.S. Gorelik, Y.Y. Pyatyshev, Raman scattering in diamond nano- and microcrystals, synthesized at high temperatures and high pressures, *Diam Relat Mater* 110 (2020). <https://doi.org/10.1016/j.diamond.2020.108104>.
- [48] A. Chepurov, S. Goryainov, S. Gromilov, E. Zhimulev, V. Sonin, A. Chepurov, Z. Karpovich, V. Afanasiev, N. Pokhilenko, HPHT-Treated Impact Diamonds from the Popigai Crater (Siberian Craton): XRD and Raman Spectroscopy Evidence, *Minerals* 13 (2023). <https://doi.org/10.3390/min13020154>.
- [49] M. Tsuda, M. Nakajima, S. Oikawa, 1137. (i) Hao, 2.; Mitura, St.; Wender, B. *Ibid.* 1983, 1143. ti) Mori, T.; Namba, Y, 1986.
- [50] H. Kawarada, *Hydrogen-terminated diamond surfaces and interfaces*, 1996.
- [51] S. Salustro, F.S. Gentile, P. D’Arco, B. Civalleri, M. Rérat, R. Dovesi, Hydrogen atoms in the diamond vacancy defect. A quantum mechanical vibrational analysis, *Carbon N Y* 129 (2018) 349–356. <https://doi.org/10.1016/j.carbon.2017.12.011>.
- [52] X. Jiang, C.L. Jia, Structure and defects of vapor-phase-grown diamond nanocrystals, *Appl Phys Lett* 80 (2002) 2269–2271. <https://doi.org/10.1063/1.1458071>.

- [53] C.-L. Cheng, H.-C. Chang, J.-C. Lin, K.-J. Song, J.-K. Wang, Direct Observation of Hydrogen Etching Anisotropy on Diamond Single Crystal Surfaces, 1997.

Figures

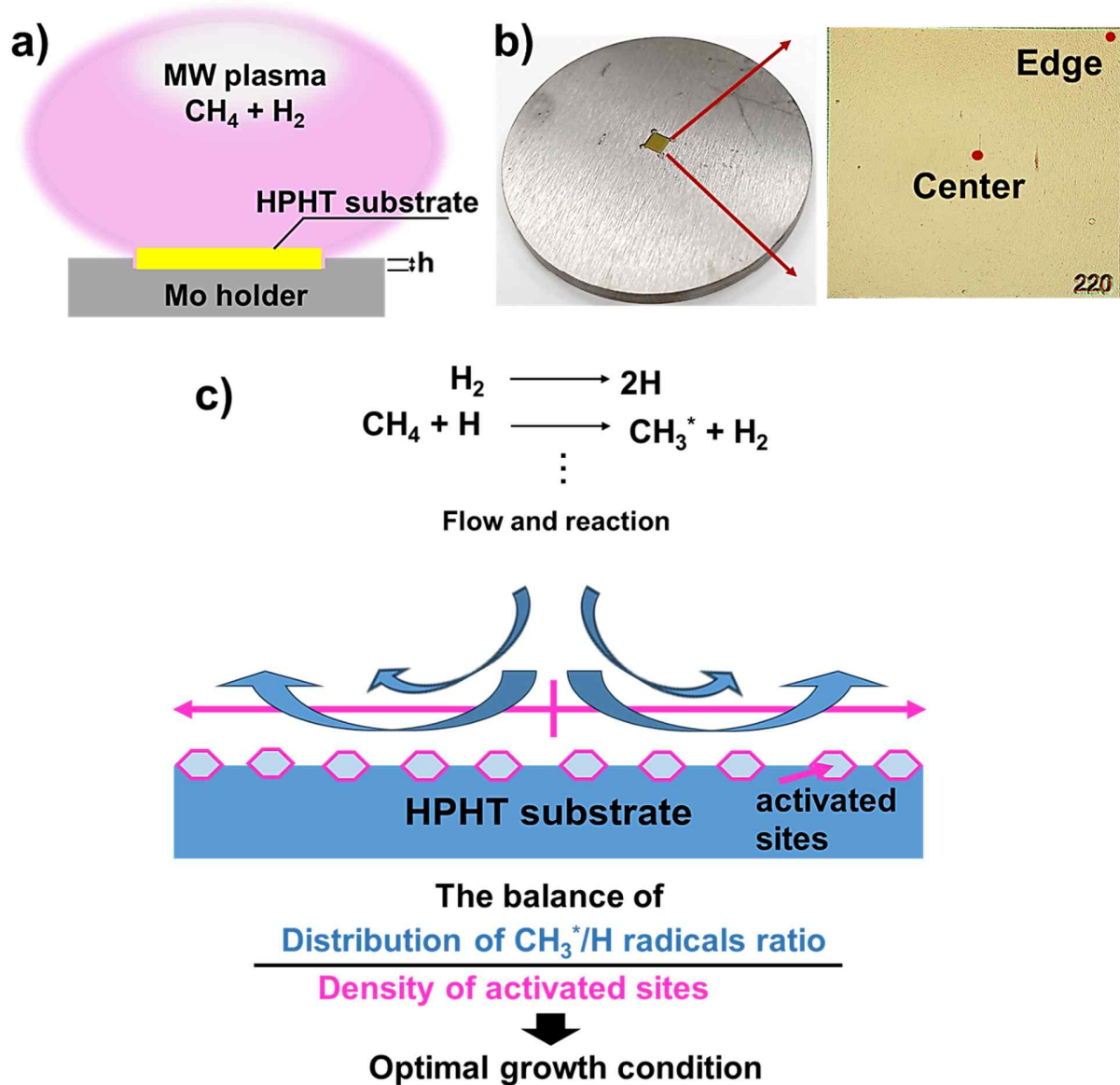


Fig. 1. Plasma-assisted CVD diamond growth process using CH₄ and H₂ gases. a) The illustration of the geometry of the Mo substrate holder. b) The image of the HPHT diamond plate on the Mo substrate holder and the marked surface of the diamond sample indicates the positions used for analysis at the center and edge of the sample. c) Schematic showing the interaction and deposition of diamond via Plasma - CVD method.

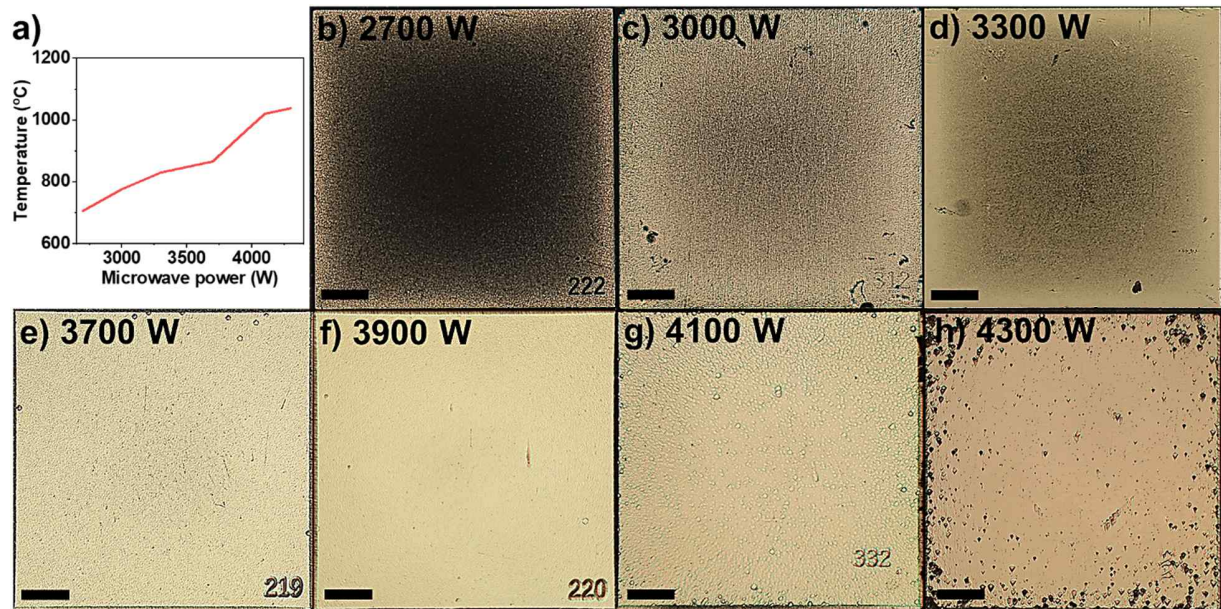


Fig. 2. (a) Diagram illustrating the relationship between the sample surface temperature and microwave power. (b-h) Optical images of the samples deposited in different microwave power conditions ranging from 2,700 W to 4,300 W, respectively at 2.5x magnification. The scale in all images is 500 μm .

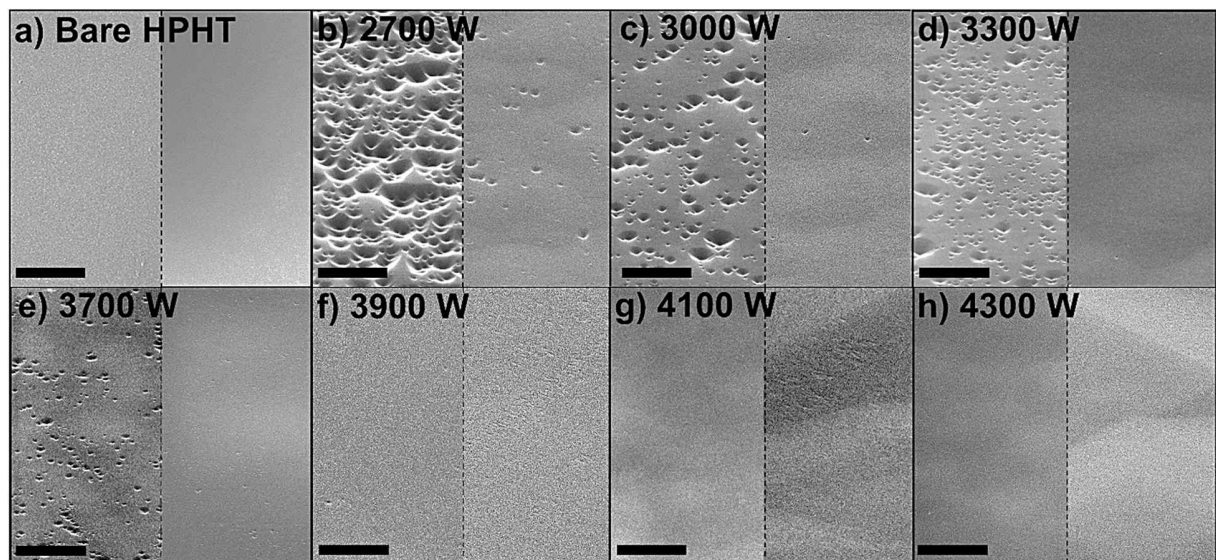


Fig. 3. SEM images of the center (left) and the edge (right) of (a) bare HPHT substrate and (b-h) of the samples deposited in different microwave power conditions ranging from 2,700 W to 4,300 W, respectively. The scale in all images is 5 μm .

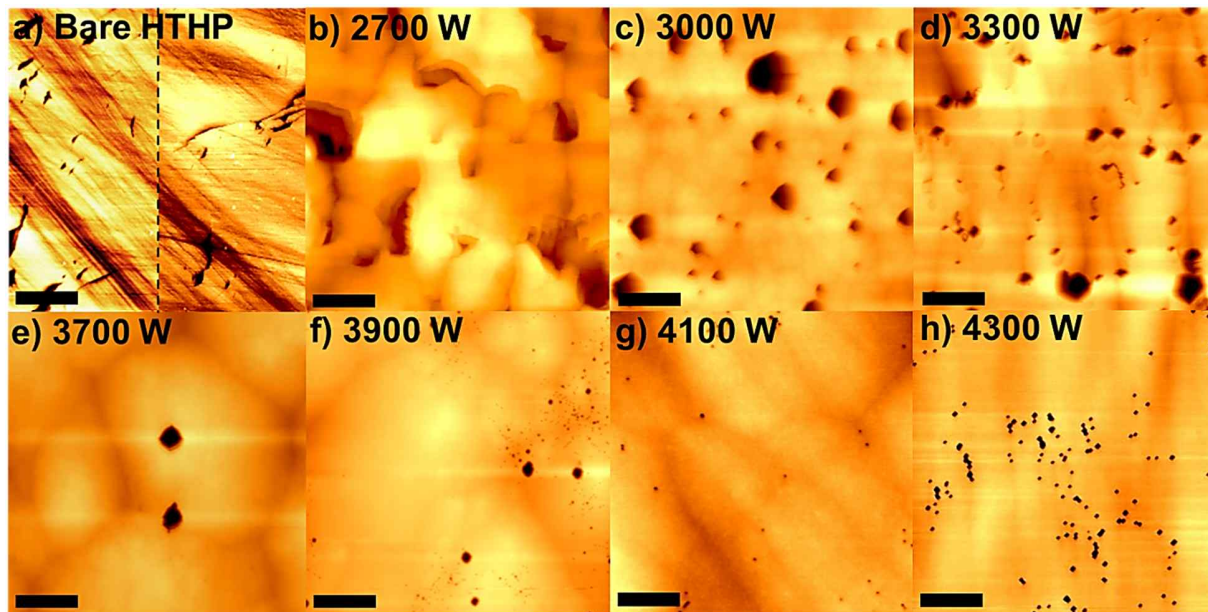


Fig. 4. AFM images of (a) bare HPHT diamond substrate at the center (left) and edge (right) and (b-h) of the samples grown in different conditions of microwave power ranging from 2,700 W to 4,300 W, respectively. The scale in all images is 2 μm .

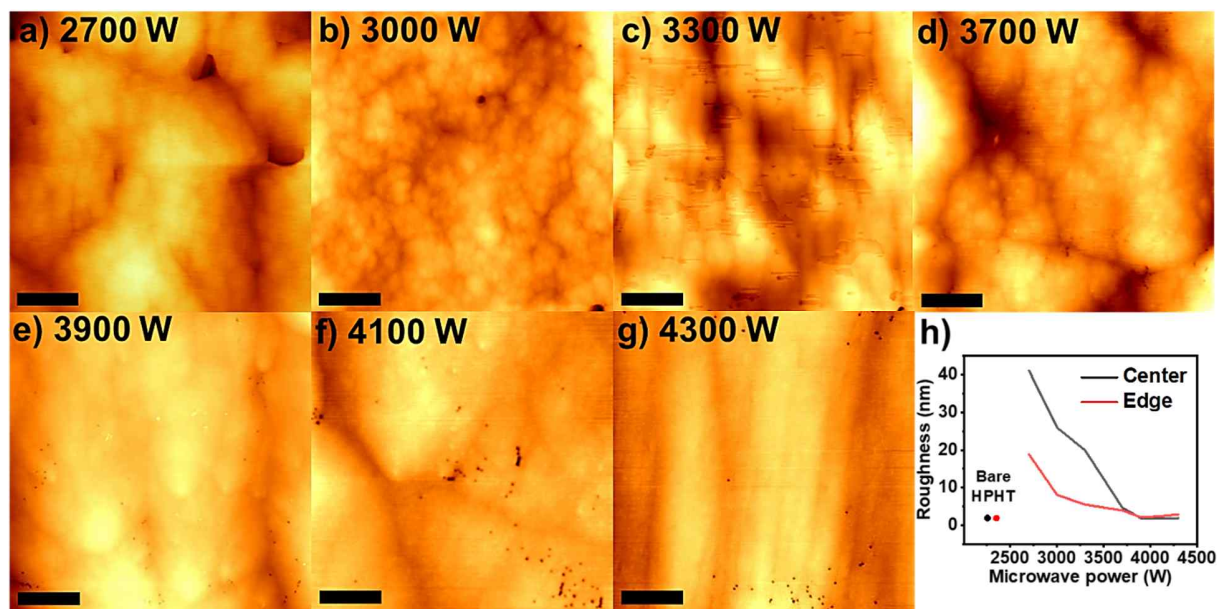


Fig. 5. (a-g) AFM images at the edge of the samples grown in different microwave power ranging from 2,700 W to 4,300 W, respectively, (h) diagram displays the relationship between the RMS roughness of sample and microwave power. The scale in all images is 2 μm .

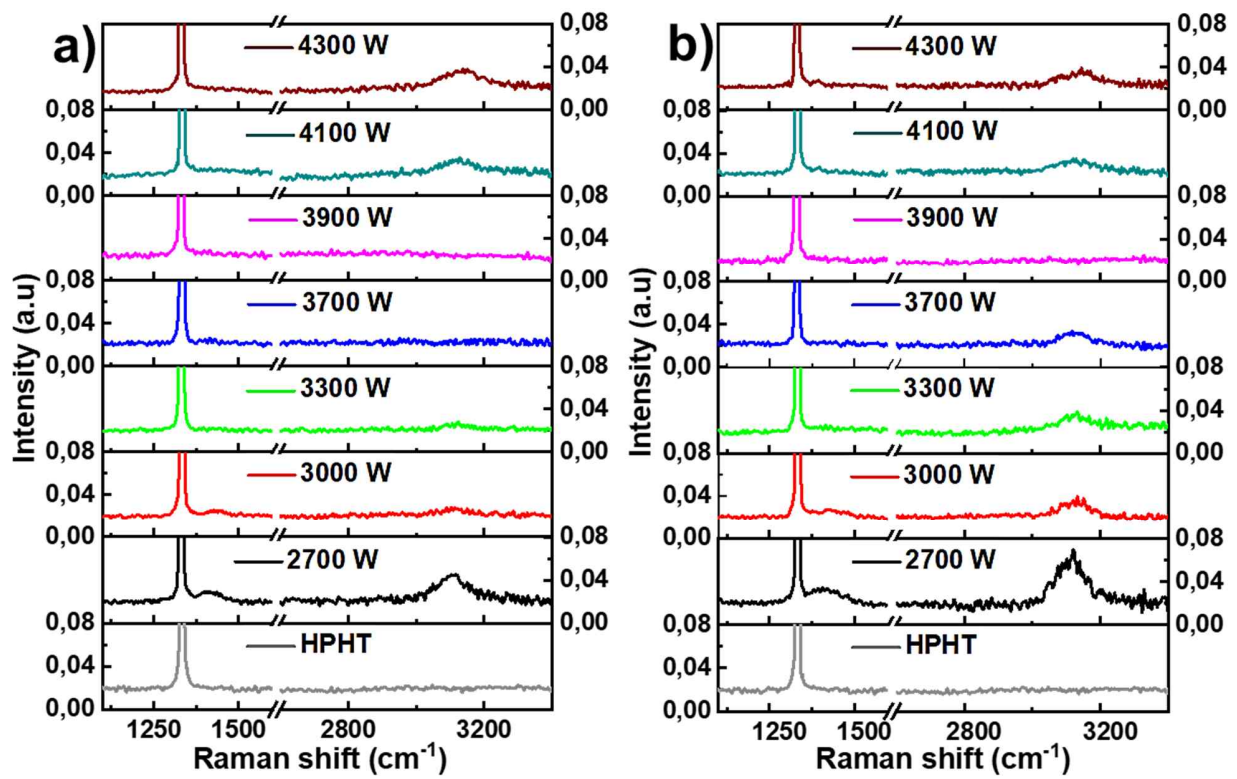


Fig 6. Raman spectra at (a) center and (b) edge of samples deposited in different conditions of microwave power ranging from 2,700 W to 4,300 W.

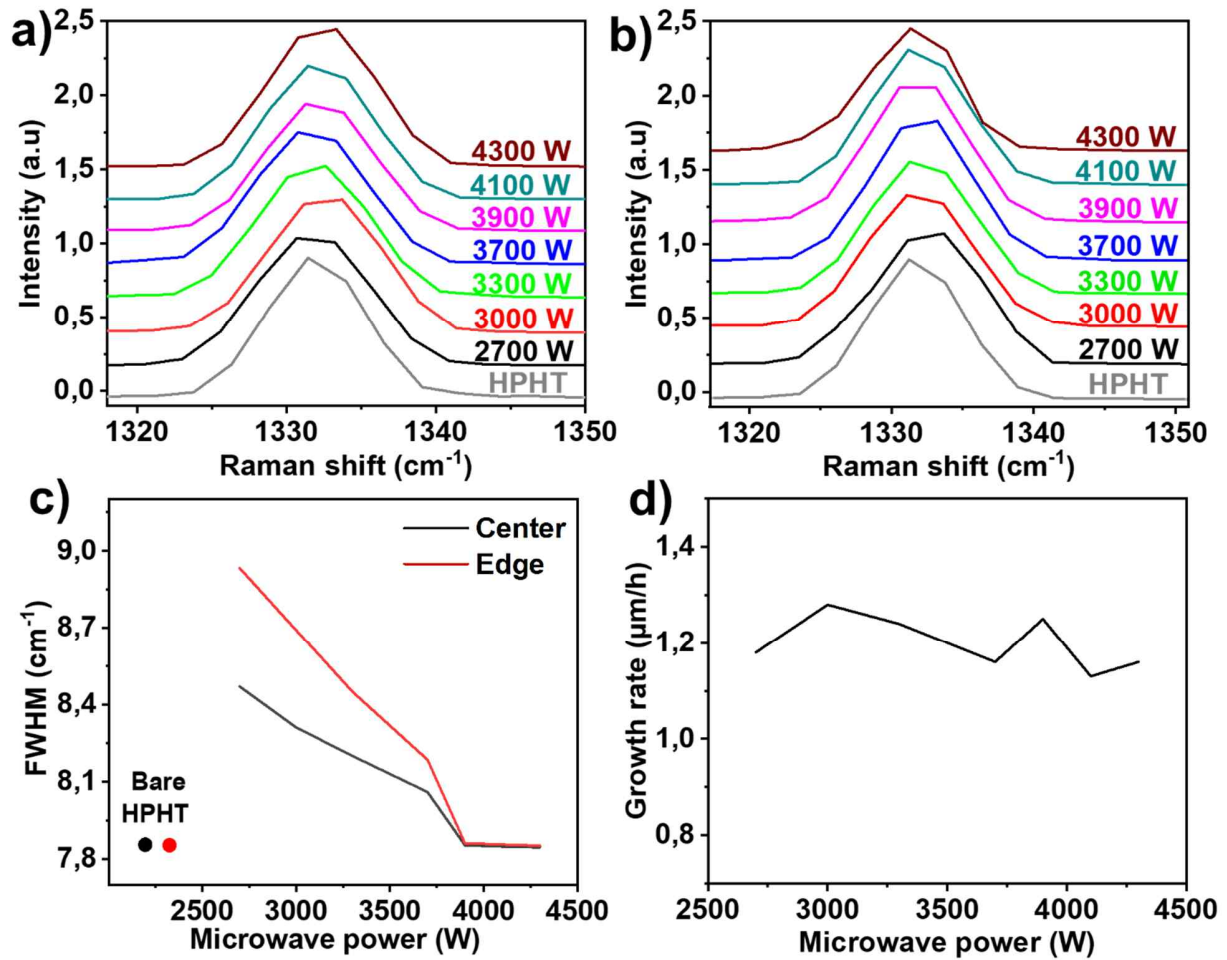


Fig 7. The single diamond peak at (a) the center and (b) the edge of samples deposited in different conditions of microwave power, (c) the comparison of FWHM of samples, and (d) the diagram reveals the relationship between the growth rate and microwave power.

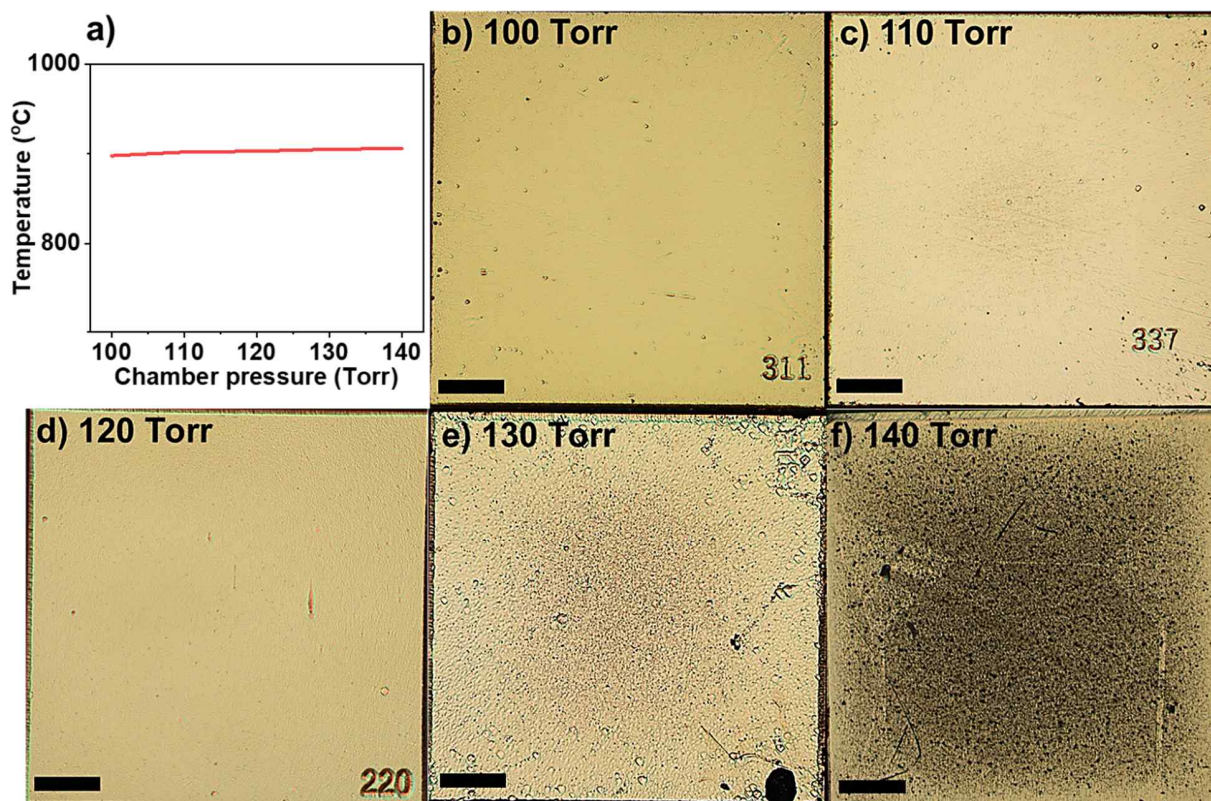


Fig. 8. (a) Diagram illustrating the sample surface temperature and chamber pressure relationship. (b-f) Optical images of the samples were deposited in different chamber pressure conditions ranging from 100 Torr to 140 Torrs, respectively, at 2.5x magnification. The scale in all images is 500 μm .

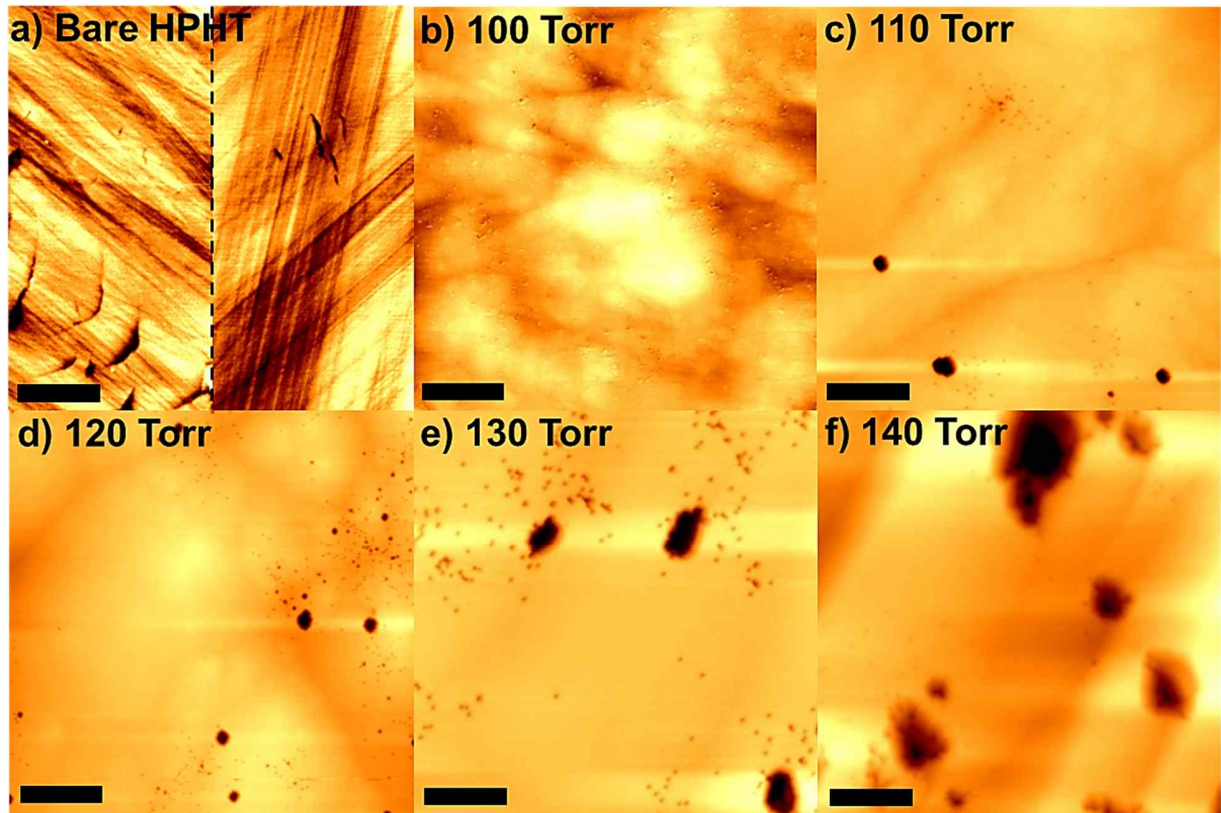


Fig. 10. AFM images of (a) bare HPHT substrate at the center (left) and edge (right) and (b-f) of the samples deposited in different chamber pressures ranging from 100 Torr to 140 Torrs, respectively. The scale in all images is 2 μm .

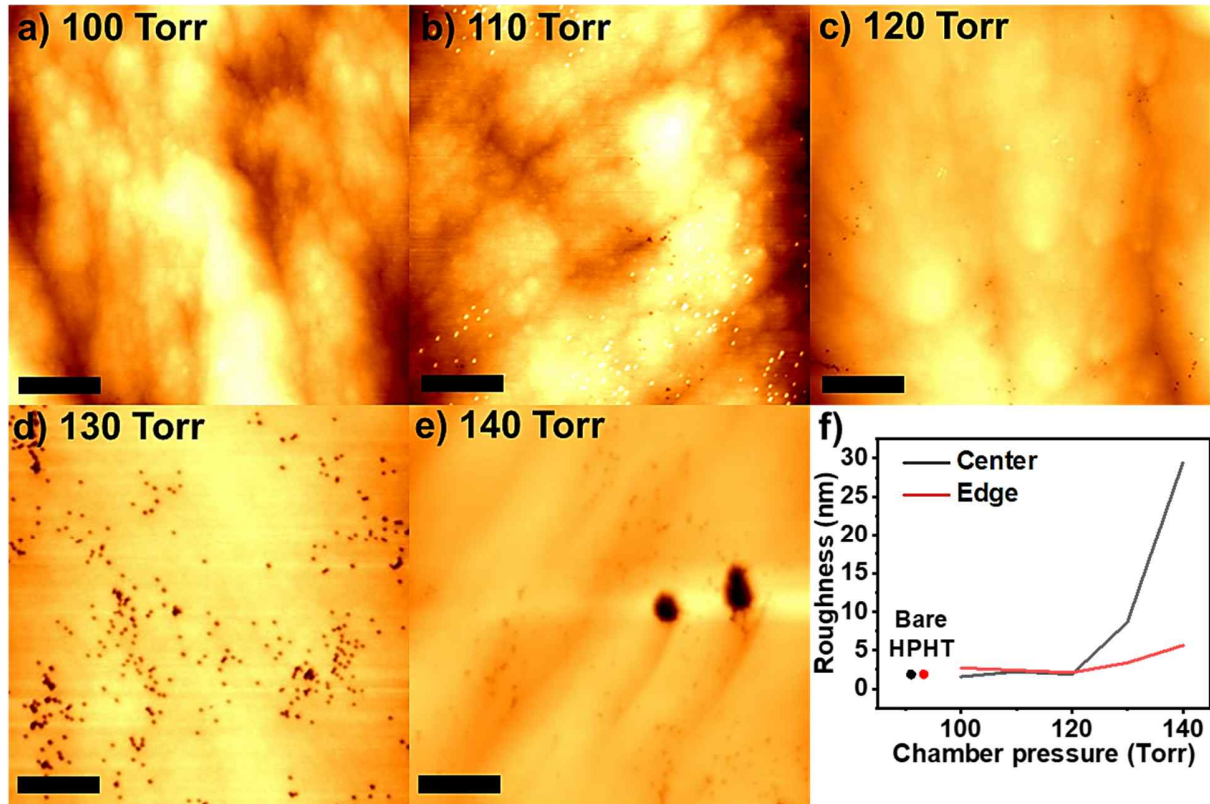


Fig. 11. (a-e) AFM images of the edge of samples deposited in different chamber pressures ranging from 100 Torr to 140 Torr, respectively, and (f) diagram displays the relationship between the RMS roughness and chamber pressure. The scale in all images is 2 μm .

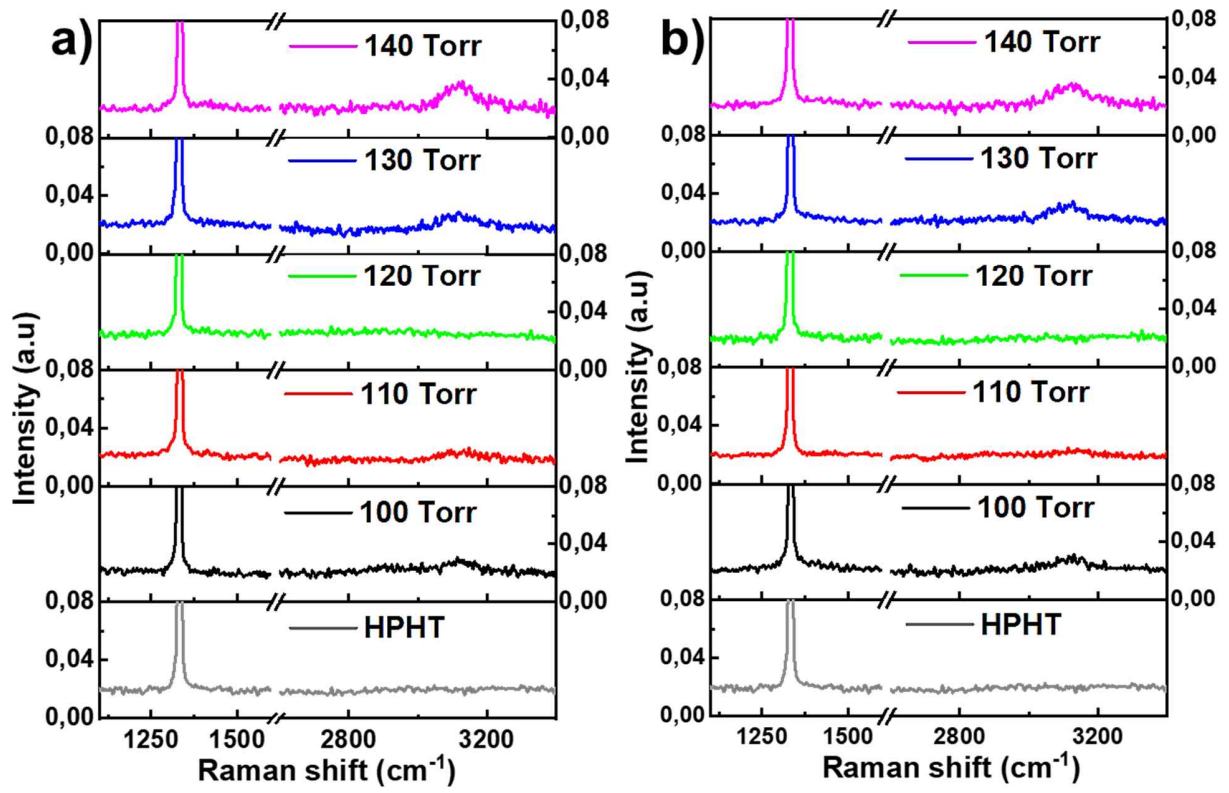


Fig. 12. Raman spectra at (a) center and (b) edge of samples deposited in different chamber pressures ranging from 100 Torr to 140 Torr.

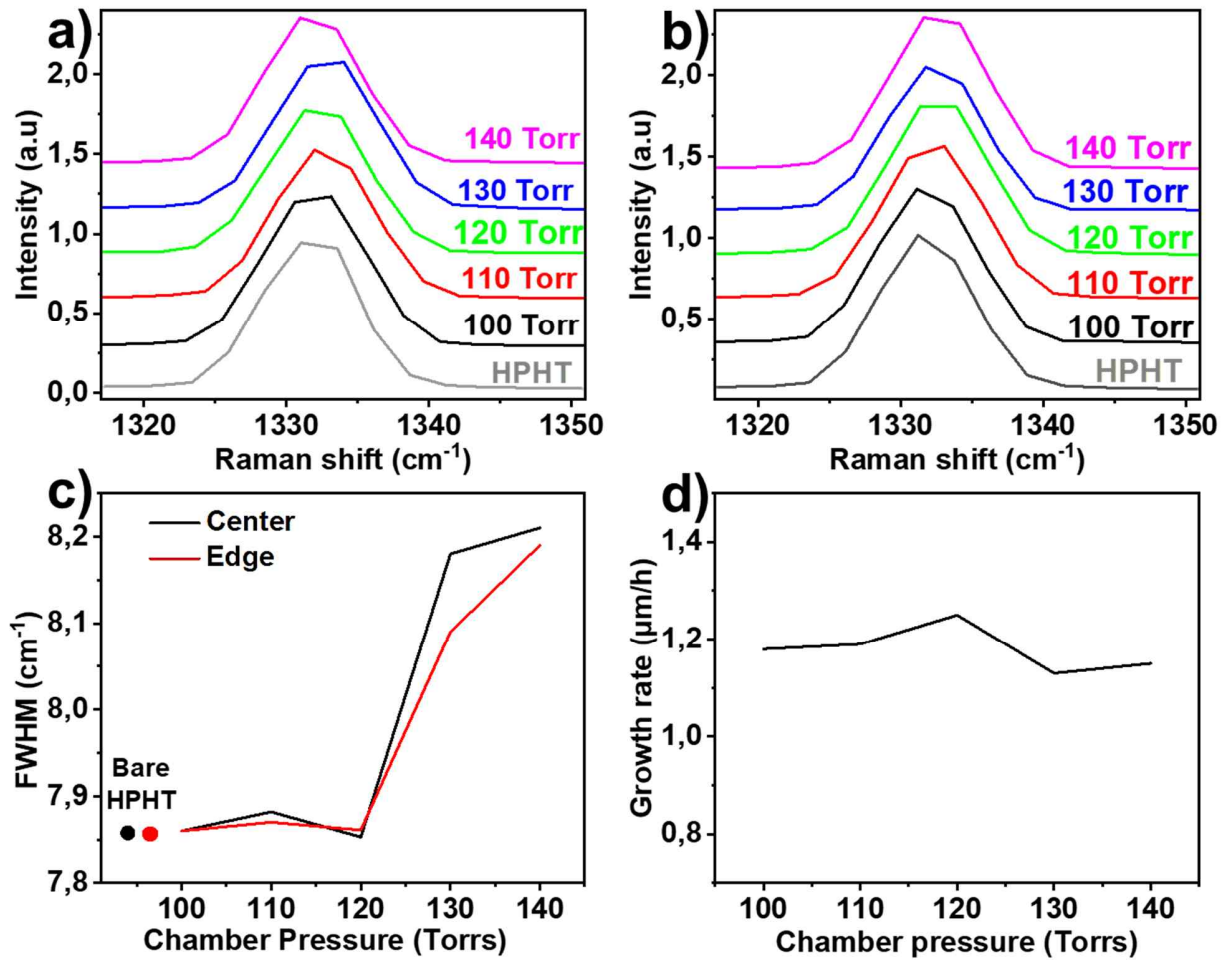


Fig. 13. The single diamond peak at (a) the center and (b) the edge of samples deposited in different conditions of chamber pressure, (c) the comparison of FWHM of samples, and (d) the diagram reveals the relationship between the growth rate and chamber pressure.